Ultra-high-accuracy Digital Terrain Model Mapping for Assessing Roadway Vulnerability to Sea-level Rise and Flooding: An Integrated Analysis of Mobile and Airborne LiDAR Data

Qi Chen, Department of Geography and Environment, University of Hawaiʻi at Mānoa

TECHNICAL REPORT DOCUMENTATION PAGE

1. Report No. PSR-UH-18-41	**2. Government Accession No.** N/A	**3. Recipient's Catalog No.** N/A

4. Title and Subtitle Ultra-high-accuracy Digital Terrain Model Mapping for Assessing Roadway Vulnerability to Sea-level Rise and Flooding: An Integrated Analysis of Mobile and Airborne LiDAR Data	**5. Report Date** September 2019	
	6. Performing Organization Code N/A	

7. Author(s) Qi Chen, PhD https://orcid.org/0000-0003-0110-7996	**8. Performing Organization Report No.** PSR-UH-18-41

9. Performing Organization Name and Address University of Hawai'i at Manoa 2500 Campus Rd Honolulu, HI 96822	**10. Work Unit No.** N/A
	11. Contract or Grant No. USDOT Grant 69A3551747109

12. Sponsoring Agency Name and Address U.S. Department of Transportation Office of the Assistant Secretary for Research and Technology 1200 New Jersey Avenue, SE, Washington, DC 20590	**13. Type of Report and Period Covered** Final Report (September 2018 – August 2019)
	14. Sponsoring Agency Code USDOT OST-R

15. Supplementary Notes N/A

16. Abstract

The transportation network along the Hawaiian coastline is vulnerable to sea-level rise (SLR) and flooding. Digital terrain models (DTMs) are a major input for assessing the vulnerability of roadways. Airborne LiDAR (Light Detection and Ranging) is widely recognized as the state-of-the-art DTM mapping technology for assessing SLR-induced inundation over relatively large areas. However, their point density is not high enough to capture the fine details of roadways such as curbs and surface water ponds. This project proposes to use mobile LiDAR data from a moving vehicle, in combination with airborne LiDAR data, to produce DTM of ultra-high accuracy for assessing the impacts of SLR and flooding. We will develop efficient algorithms and a methodological framework that can combine the strengths of both airborne and mobile LiDAR data to generate precise and detailed DTMs. The DTMs generated from the combined LiDAR data will be compared against the DTMs from only airborne LiDAR data to examine the benefits of introducing mobile LiDAR data in inundation analysis. A watershed-level DTM will also be generated by integrating DTMs from airborne LiDAR, mobile LiDAR, and photogrammetry, which can be used by hydrologists for simulating the impacts of flooding on roadway infrastructure. This pilot study will provide useful recommendations regarding how to use the state-of-the-art LiDAR technologies for assessing the risk of transportation network to SLR and flooding over coastal areas.

17. Key Words Flooding, sea-level, transportation management, mapping, terrain evaluation	**18. Distribution Statement** No restrictions.

19. Security Classif. (of this report) Unclassified	**20. Security Classif. (of this page)** Unclassified	**21. No. of Pages** 33	**22. Price** N/A

Form DOT F 1700.7 (8-72)   Reproduction of completed page authorized

PSR Pacific Southwest Region UTC
University Transportation Center

TABLE OF CONTENTS

Pacific Southwest Region UTC
University Transportation Center

About the Pacific Southwest Region University Transportation Center

The Pacific Southwest Region University Transportation Center (UTC) is the Region 9 University Transportation Center funded under the US Department of Transportation's University Transportation Centers Program. Established in 2016, the Pacific Southwest Region UTC (PSR) is led by the University of Southern California and includes seven partners: Long Beach State University; University of California, Davis; University of California, Irvine; University of California, Los Angeles; University of Hawaii; Northern Arizona University; Pima Community College.

The Pacific Southwest Region UTC conducts an integrated, multidisciplinary program of research, education and technology transfer aimed at *improving the mobility of people and goods throughout the region.* Our program is organized around four themes: 1) technology to address transportation problems and improve mobility; 2) improving mobility for vulnerable populations; 3) Improving resilience and protecting the environment; and 4) managing mobility in high growth areas.

U.S. Department of Transportation (USDOT) Disclaimer

The contents of this report reflect the views of the authors, who are responsible for the facts and the accuracy of the information presented herein. This document is disseminated in the interest of information exchange. The report is funded, partially or entirely, by a grant from the U.S. Department of Transportation's University Transportation Centers Program. However, the U.S. Government assumes no liability for the contents or use thereof.

Disclosure

Principal Investigator, Co-Principal Investigators, others, conducted this research titled, "Ultra-high-accuracy Digital Terrain Model Mapping for Assessing Roadway Vulnerability to Sea-level Rise and Flooding: An Integrated Analysis of Mobile and Airborne LiDAR Data" at the Department of Geography and Environment, University of Hawai'I at Manoa. The research took place from September 1, 2018 to August 31, 2019 and was funded by a grant from the US Department of Transportation in the amount of $19,988. The research was conducted as part of the Pacific Southwest Region University Transportation Center research program.

Pacific Southwest Region UTC
University Transportation Center

Abstract

The transportation network along the Hawaiian coastline is vulnerable to sea-level rise (SLR) and flooding. Digital terrain models (DTMs) are a major input for assessing the vulnerability of roadways. Airborne LiDAR (Light Detection and Ranging) is widely recognized as the state-of-the-art DTM mapping technology for assessing SLR-induced inundation over relatively large areas. However, their point density is not high enough to capture the fine details of roadways such as curbs and surface water ponds. This project proposes to use mobile LiDAR data from a moving vehicle, in combination with airborne LiDAR data, to produce DTM of ultra-high accuracy for assessing the impacts of SLR and flooding. We will develop efficient algorithms and a methodological framework that can combine the strengths of both airborne and mobile LiDAR data to generate precise and detailed DTMs. The DTMs generated from the combined LiDAR data will be compared against the DTMs from only airborne LiDAR data to examine the benefits of introducing mobile LiDAR data in inundation analysis. A watershed-level DTM will also be generated by integrating DTMs from airborne LiDAR, mobile LiDAR, and photogrammetry, which can be used by hydrologists for simulating the impacts of flooding on roadway infrastructure. This pilot study will provide useful recommendations regarding how to use the state-of-the-art LiDAR technologies for assessing the risk of transportation network to SLR and flooding over coastal areas.

Pacific Southwest Region UTC
University Transportation Center

Introduction

The Hawaiian archipelago is vulnerable to multiple hazards and threats, among which are sea-level rise (SLR) and flooding (Fletcher et al., 2010; Onat et al., 2018). The SLR, in the events of flash flood and storm surges, can escalate coastal erosion and increase infrastructure damage (Onat et al., 2018). The 2017 Hawai'i Sea Level Rise Vulnerability and Adaptation (HSLRVA) report (HCCMAC, 2017) suggested that a 3.2 feet of projected SLR is possible in the state over this century. The SLR-induced chronic flooding would make 25,800 acres of land unusable, compromise or lose over 6,500 structures, and result in economic loss of $19 billion for the flooded structure and associated land. The full potential loss may amount to an order of magnitude greater, due to such consequences as the erosions of iconic beaches, the flooding of sewage disposal systems, and the loss of native species and ecosystem services (HCCMAC, 2017).

One type of critical infrastructure that can be also severely impacted by SLR and flooding is transportation. The 2017 HSLRVA report projected that over 38 miles of major roads will be chronically flooded with 3.2 feet of sea-level rise. In Oahu, low-lying land is very limited and utilities such as water, wastewater, and electrical systems often run besides or beneath roadways (HCCMAC, 2017). Therefore, the cost for repairing and relocating vulnerable roadways, even for short distance, is vastly large. Digital terrain models (DTMs), as a major input for simulating hydrological processes, play a key role in improving our understanding of the SLR and flooding risk of roadways and developing cost-effective mitigation and adaption plans.

Airborne LiDAR (Light Detection and Ranging) remote sensing has been widely recognized as the state-of-the-art DTM mapping technology for studying SLR and simulating flooding events over relatively large areas (Yin et al., 2017). For example, Gesch (2009) compared three types of elevation models of different spatial resolutions (1 km, 90 m, and 30 m) with LiDAR-derived high spatial resolution (3 m) DTM to map the potential inundation areas due to SLR in North Carolina. He found that the area of inundation can differ by a factor of 3-4 due to the use of different elevation models and thus suggested the use of airborne LiDAR for coastal area SLR analysis at the national level. In recent years, airborne LiDAR has also been used for SLR studies in Hawaii (Cooper et al., 2013 a,b; Cooper and Chen, 2013).

However, no research has been done yet for using LiDAR technology to specifically assess the roadway infrastructure vulnerability to SLR and flooding. Airborne LiDAR data are ideal for mapping DTM at the landscape level. Nevertheless, their typical point spacing is 30-50 cm, which is not small enough to capture detailed road features such as curbs and surface water ponds. Fortunately, the emergence of mobile LiDAR technology on a moving vehicle makes it possible to address such challenges because of its close scanning range and extremely high point density with up to 5 cm or even finer point spacing (Figure 1).
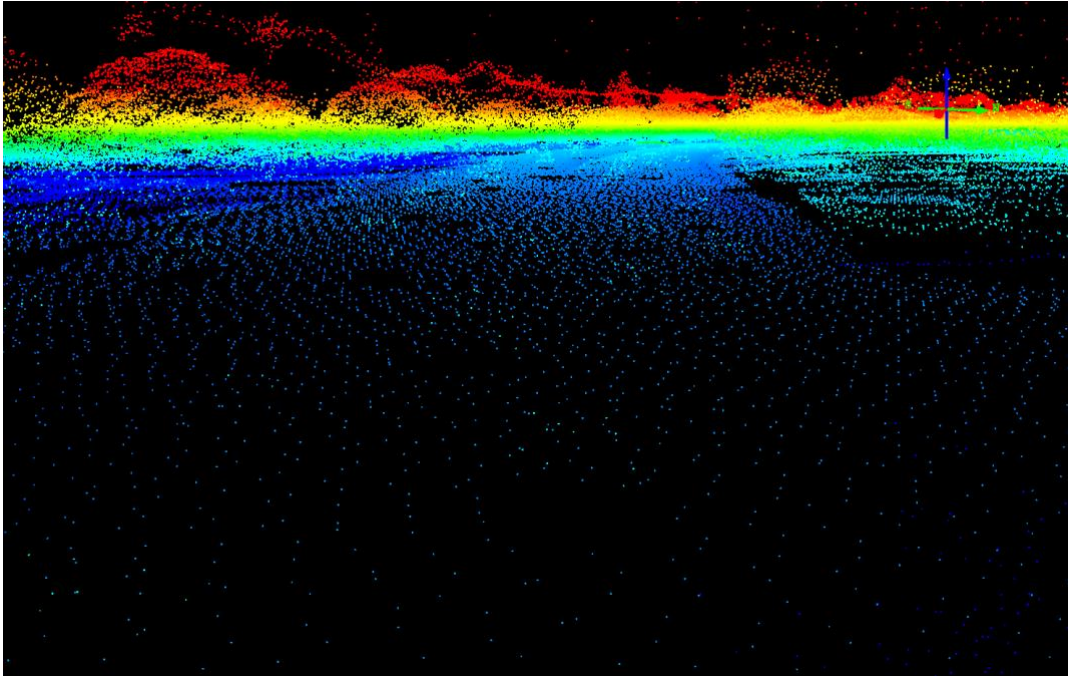
(a) airborne LiDAR
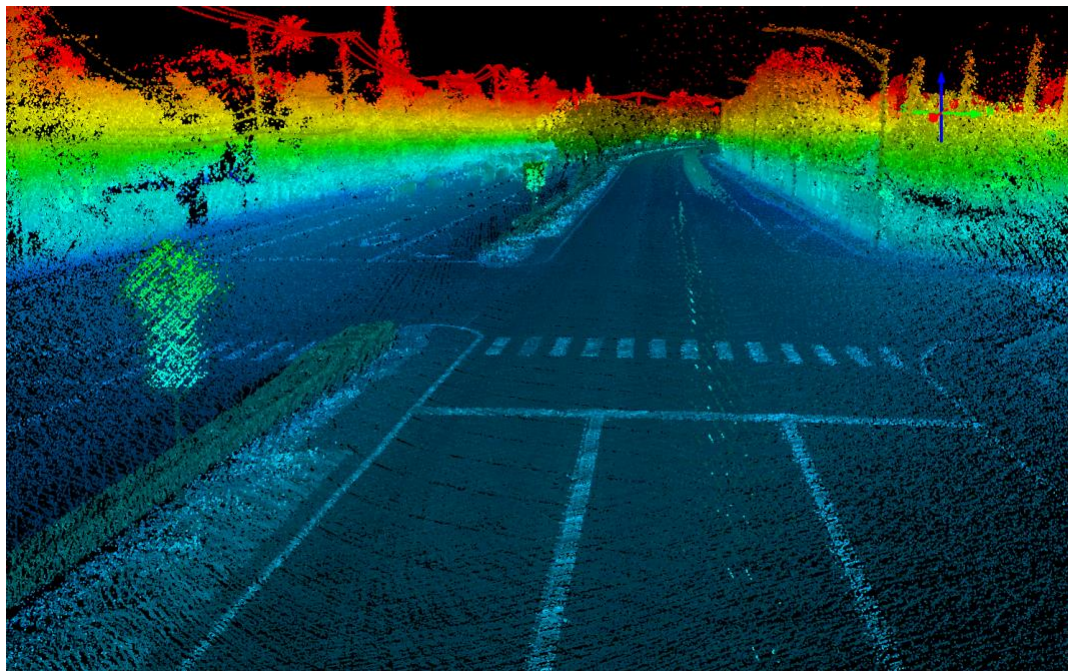
(b) mobile LiDAR

Figure 1. Comparison of airborne and mobile LiDAR data of the same area

Yet, mobile LiDAR has a few barriers for its boarder applications in detailed SLR and flooding analysis: 1) the ultra-high point density of mobile LiDAR data comes with the expense of large file size (in the order of Gigabytes every mile of data), which makes it notoriously difficult to

process, 2) the positioning and orientation systems (POS) of mobile LiDAR systems are usually not as advanced as the ones in airborne LiDAR systems, so the absolute georeferencing accuracy of mobile LiDAR data is not as high as airborne LiDAR data, and 3) mobile LiDAR, despite its high sampling density over roadways, is not able to map out-of-the-sight terrain beyond the roadways due to occlusions caused by buildings and trees; in contrast, airborne LiDAR scanning from a high vantage point can more easily have a complete coverage over a large geographical extent. Therefore, airborne and mobile LiDAR each have their own strengths and drawbacks, making them highly complementary for mapping.

The main goal of this project is to develop an integrative methodology that can maximize the advantages of both airborne and mobile LiDAR data in order to produce ultra-high accuracy DTM maps for assessing roadway vulnerability to SLR and flooding. The resulted DTM from the integrated airborne and mobile LiDAR data will be compared against the conventional DTM from airborne LiDAR data alone for SLR-related inundation analysis. A secondary goal and product of this project is that we will generate a DTM for a watershed from mountain to sea by integrating DTM from airborne LiDAR, mobile LiDAR, and conventionally photogrammetry, which can be used for a baseline dataset for simulating flooding events and its associated transportation impact analysis by hydrologists.

Mobile LiDAR System

In recent years, the Hawaii Department of Transportation (HDOT) has contracted to Mandli Communications, Inc to acquire statewide mobile LiDAR data for assisting transportation planning and management.

Figure 2. The basic components of mobile LiDAR system: 1) dual Velodyne HDL-32 LiDAR sensors, 2) nine 8.9 MP cameras, 3) position orientation system, including GNSS, Inertial Measurement Unit (IMU) and optical Distance Measurement Instrument (DMI). (Modified from Mandli Communcations, Inc)

The data used in this study were collected in 2016 with the Mandli DVX system. The system includes two Velodyne HDL-32 LiDAR sensors (each with a pulse rate of 700,000 points per second, range of 100 m, relative positive accuracy of < 2 cm for 1 sigma at 25 m, vertical angular resolution of 1.33°, wavelength of 905 nm), which are mounted at the two rear corners of the vehicle. The LiDAR sensors are oriented so they produce slightly overlapping point clouds to minimize shadows and data gaps from obstructions. The two point clouds are seamlessly combined and synchronized via GPS time-synchronization. For position and orientation, Mandli vehicles are equipped with the iXblue Atlans-C GNSS receiver (called rover) and inertial measurement unit (IMU) that record global position and inertial measurements for accurate GPS time-synchronization. The Atlans GNSS/INS (Inertial navigation system) post-processing software utilizes publicly available GNSS observation data from the National Oceanic and Atmospheric Administration's (NOAA) National Geodetic Survey (NGS) Continuously Operating Reference Stations (CORS) network for differential correction. CORS provides consistent carrier phase and code range measurements to support three-dimensional positioning.

Typically, GNSS rover signal is lost temporarily when traveling under a bridge structure or through multi-pathing in urban canyons. Given that the CORS network is not affected by these sources of error, the system used a Smoothed Best Estimate Trajectory (SBET) solution to correct the rover position and orientation. These systems constrain potential vehicle velocity and displacement errors, which allows for more accurate mapping of assets and their geographic coordinates, in case of obstructions in urban areas, canyons, and tunnels. The Mobile Mapping system allows for complete data acquisition of roadway features in a single pass at highway speeds. Road assets such as street signs, bridges, guardrails, utility poles are fully visible and accurately represented for analysis and inventory. Vehicles do not require constant stops for manual surveillance that would interrupt or halt both traffic and pedestrians walking.

3. Study Area and LiDAR Data

We develop and test our methodology by focusing on an area in east Oahu (Figure 2). This area is chosen because i) it includes the Kamehameha Highway, the only and major backbone of connecting urban Honolulu with east Oahu, and ii) according to the 2017 HSLRVA report, the Kamehameha Highway is in particular under risk of SLR.
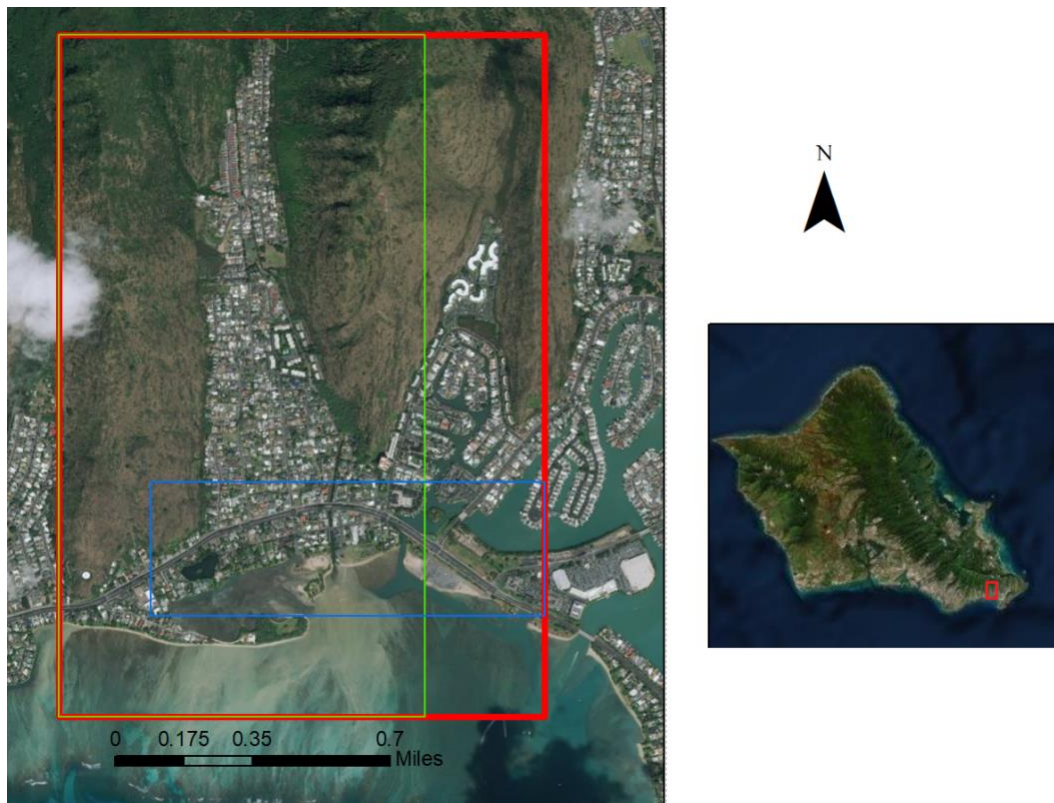
Figure 3. The study area. Green box is the bounding area of airborne LiDAR data; blue box is the bounding area of mobile LiDAR data; red box is the bounding area of both.

We used airborne LiDAR data collected by NOAA in 2013 and the mobile LiDAR data collected by Hawaii DOT in 2016 (Figure 4).
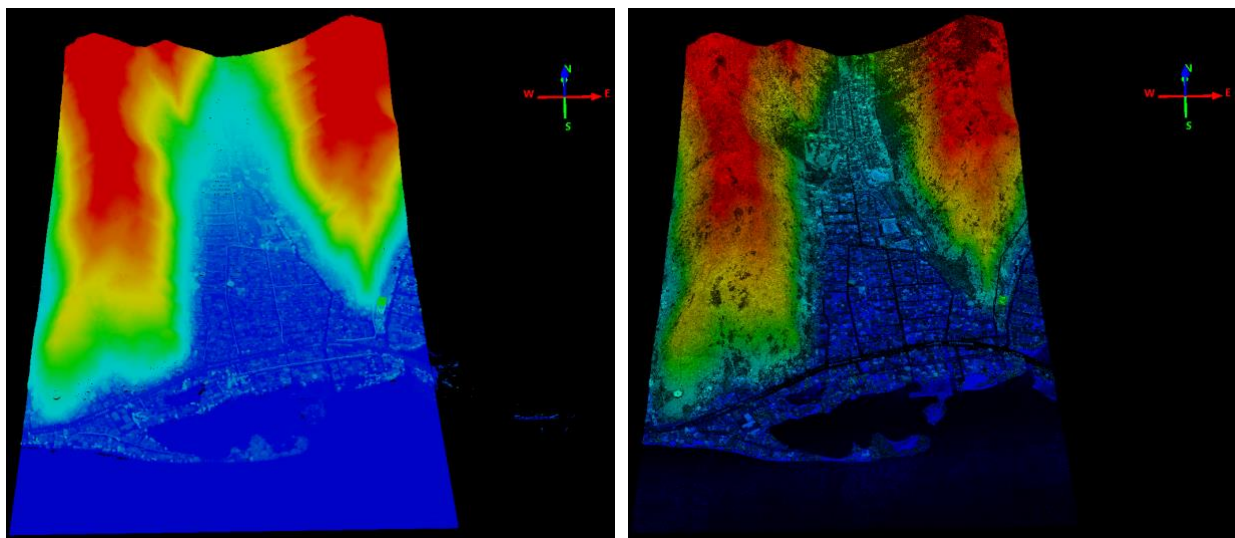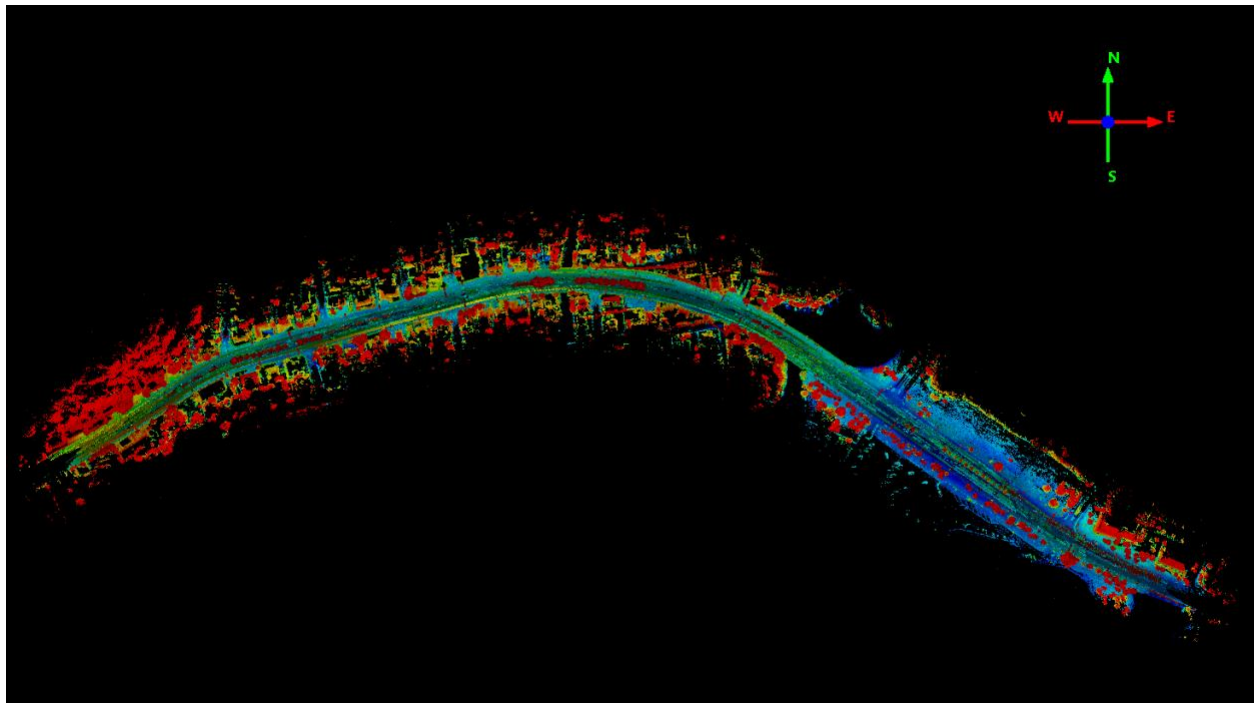
Figure 4. Visualization of airborne and mobile LiDAR data over study area. (Upper left) airborne and mobile data; rendered with elevation only, (Upper right) airborne and mobile data; rendered with both elevation and intensity values; (Bottom) mobile data; rendered with both elevation and intensity values.

For the mobile LiDAR data, we used the data collected from both the east and westward directions (Figure 5). Table 1 shows the basic statistics of all LiDAR data.
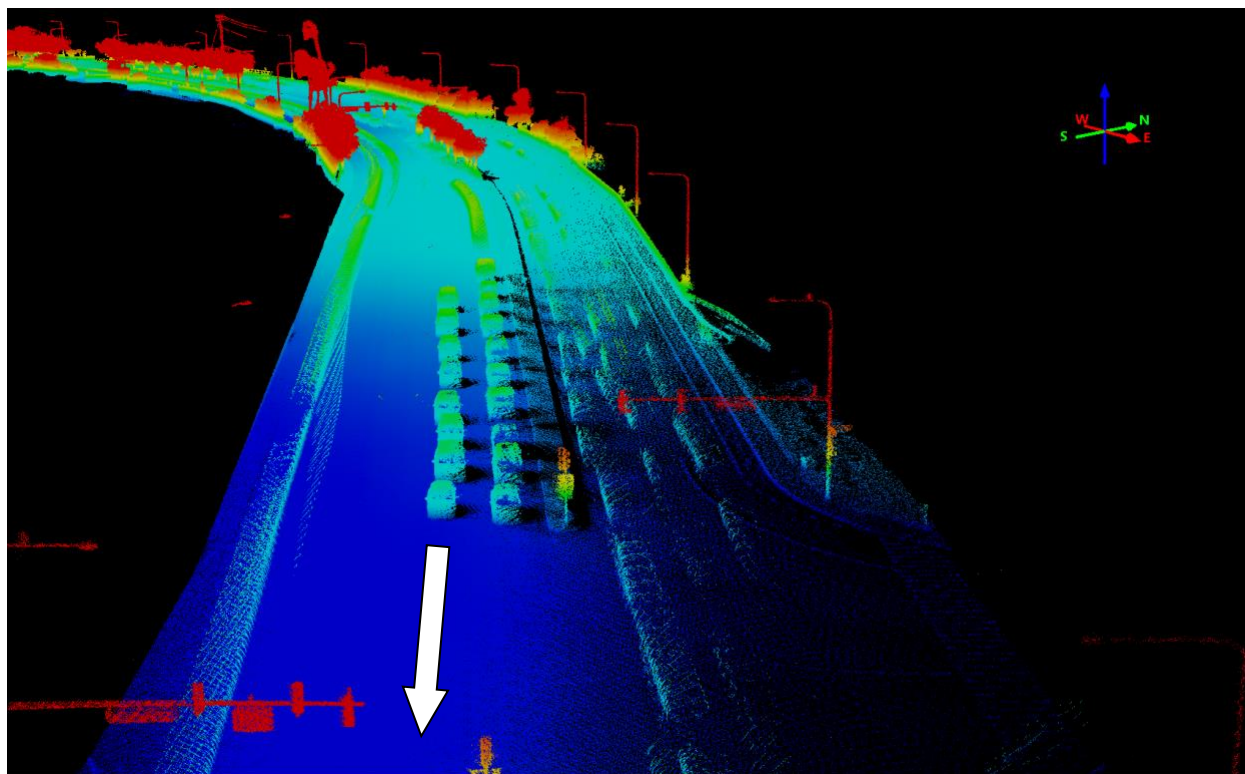
(a)   Eastward driving direction
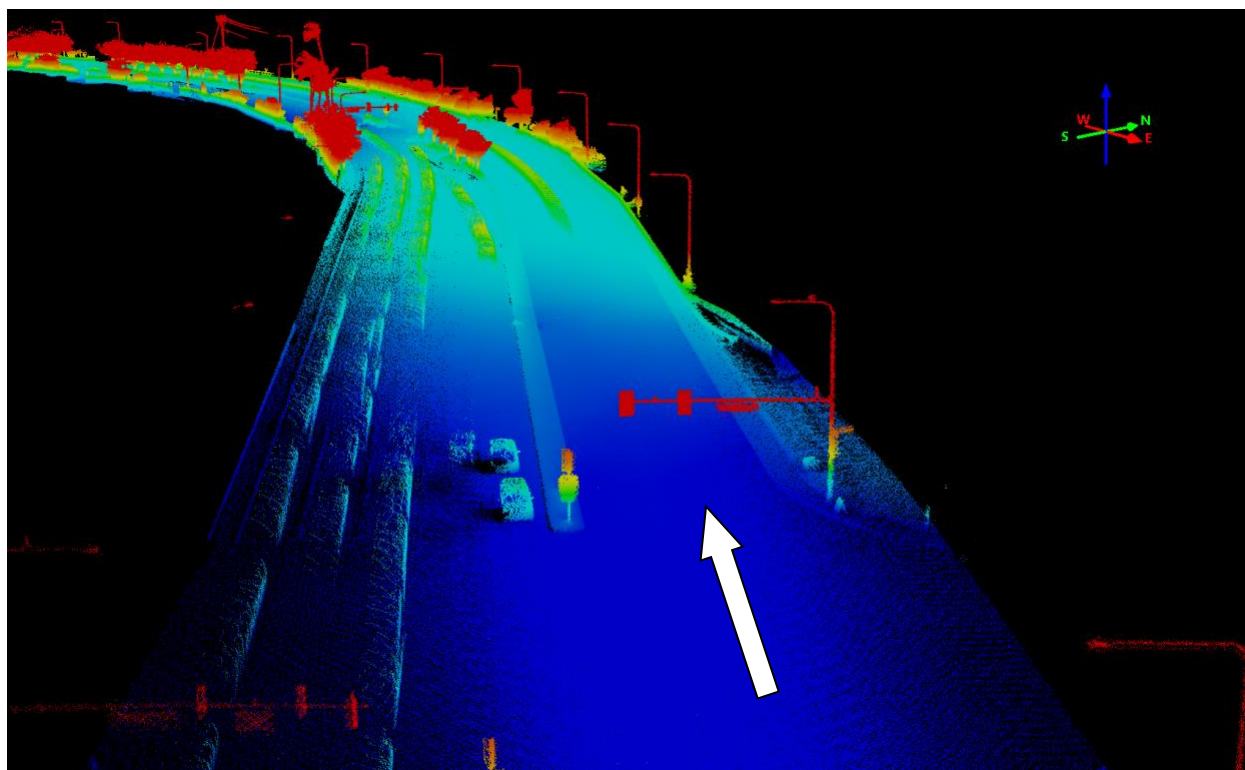
(b)   Westward driving direction

Figure 5. Visualization of mobile LiDAR data from both driving directions.

Data	File size	Number of points	Point density ($m_2/2$)	Point spacing (m)
Airborne LiDAR	273 Mb	10,254,445	2.5	0.63
Mobile LiDAR	3.81 Gb	204,605,738	3334.4	0.02

Table 1. Summary statistics of the LiDAR data.

4. Methodology

4.1. Reducing geometric errors associated with mobile LiDAR data

Even though the mobile LiDAR data have very dense point cloud (Table 1), several sources of geometric errors have been identified.

First, the Velodyne HDL-32 is a sensor with 32 channels (beams) (Figure 6). The data collected from different beams could have small discrepancy. Second, the two Velodyne sensors from the left and right rear corners (see Figure 7 for an example) of the vehicles are not necessarily perfectly calibrated. As a result, geometric errors exist in the mobile LiDAR data even when the mobile LiDAR data are collected within a short time interval (so the GNSS signals and the positional solution are relatively consistent) along one driving direction.
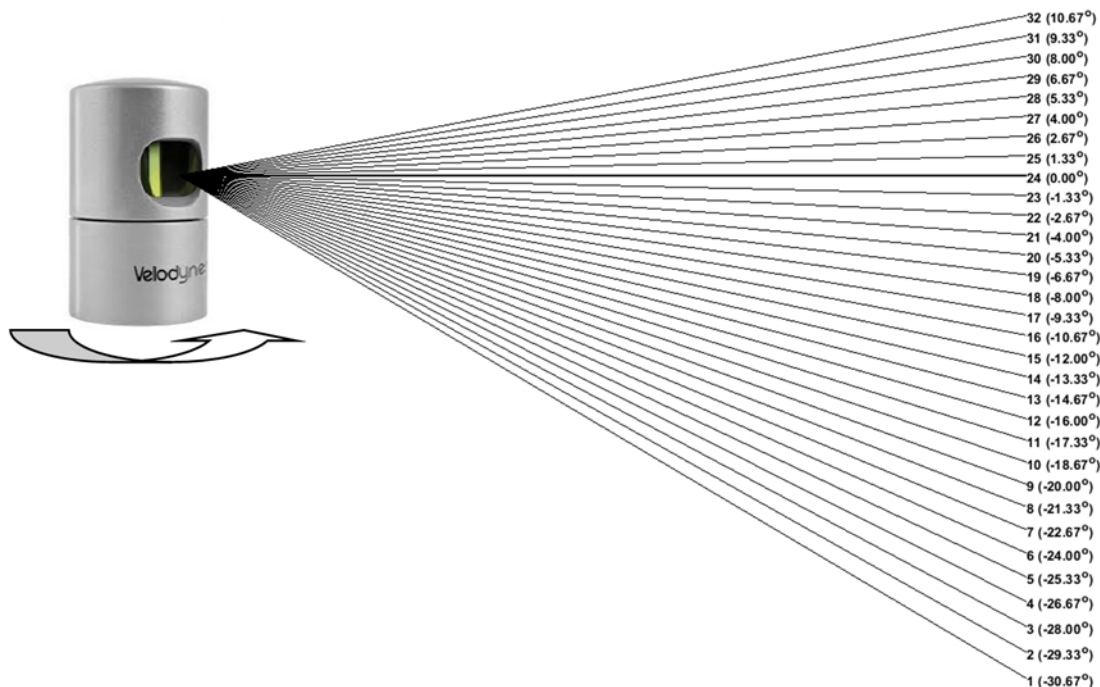
Figure 6. Beam configuration of the Velodyne HDL-32 sensor. Each line represents a different channel (beam) with different scanning angles.

Figure 7. Configuration of two Velodyne sensors on a vehicle. (Image Credit: Mandli Communications Inc).

Figure 8 shows a comparison of the point clouds (in top-down views) of a building wall from a single channel of a single sensor and all channels of the two sensors. I found that the geometric errors associated with the use of different channels and the two sensors are about 20 cm.
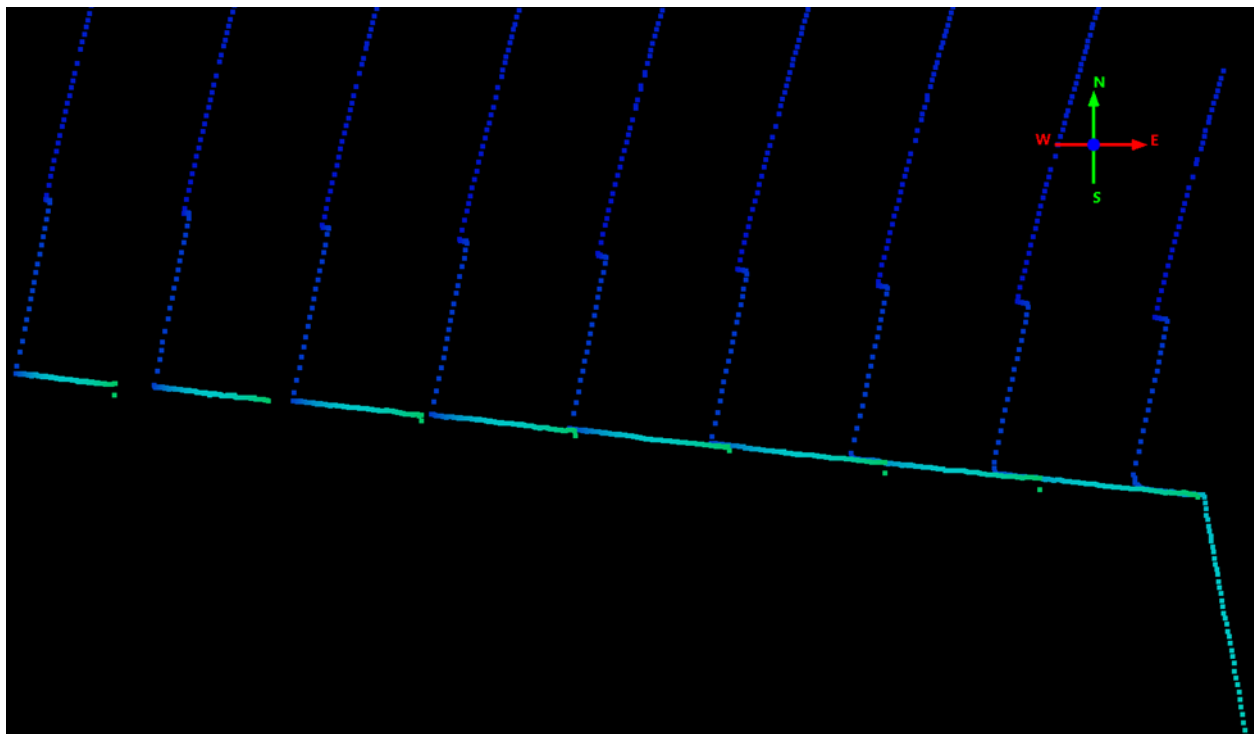
(a)
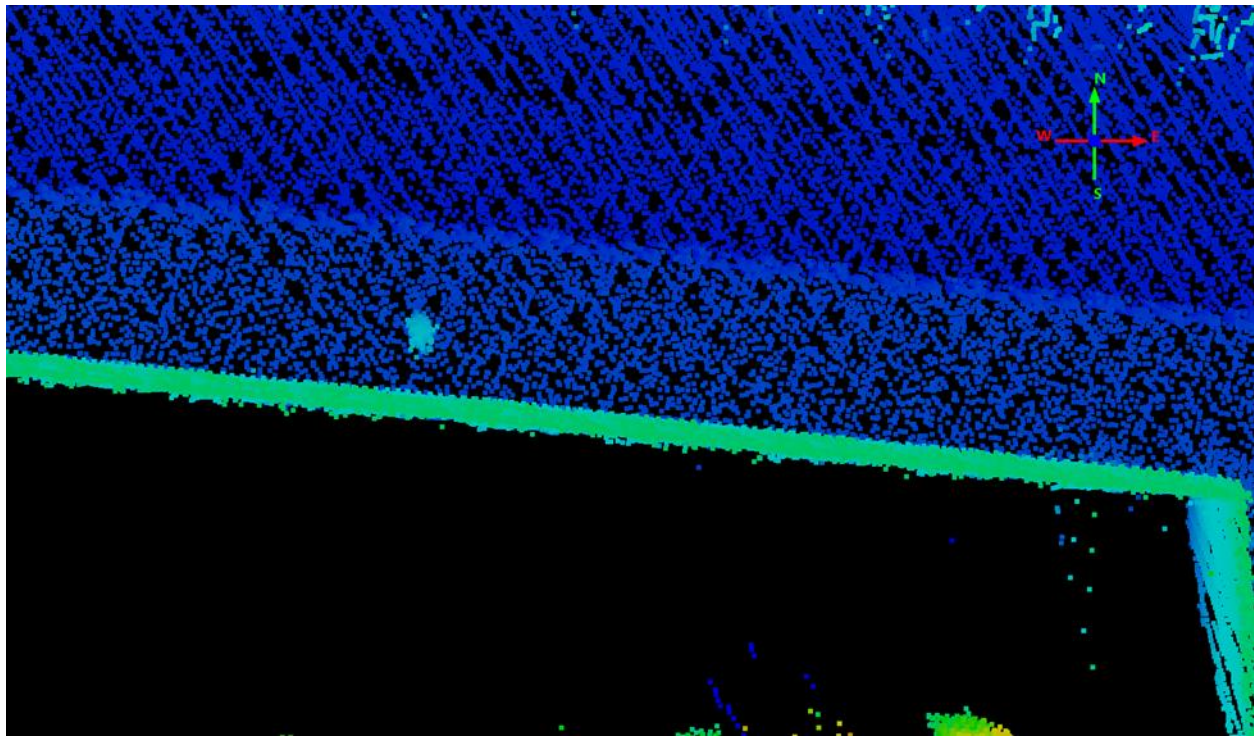
(b)

Figure 8. Geometric errors associated with different beams and the two Velodyne sensors. Shown are the top-down views of a wall from the data of (a) one channel of a Velodyne sensor, and (b) all channels of two Velodyne sensors.

Additional geometric errors are associated with the use of mobile LiDAR data collected from different driving directions. The eastward and westward mobile LiDAR data are collected at different times, which could differ by tens of minutes or hours. The GNSS satellite spatial configurations vary over time, which leads to difference in the corresponding positioning solutions even over the same locations. Figure 9 shows an example area of 2 m by 1m over a road surface: the point clouds from the eastward and westward driving directions are systematically different with a vertical difference about 0.215 meter over the small area. For the whole dataset and the study area, I calculated the nearest distance from any point in the eastward point cloud to the westward point cloud (Figure 10) and found that: 1) the systematic difference between the point clouds are not constant, and 2) a large portion of the area have a difference of 0.3 m or more.

(a)

Difference = 0.215 Meters
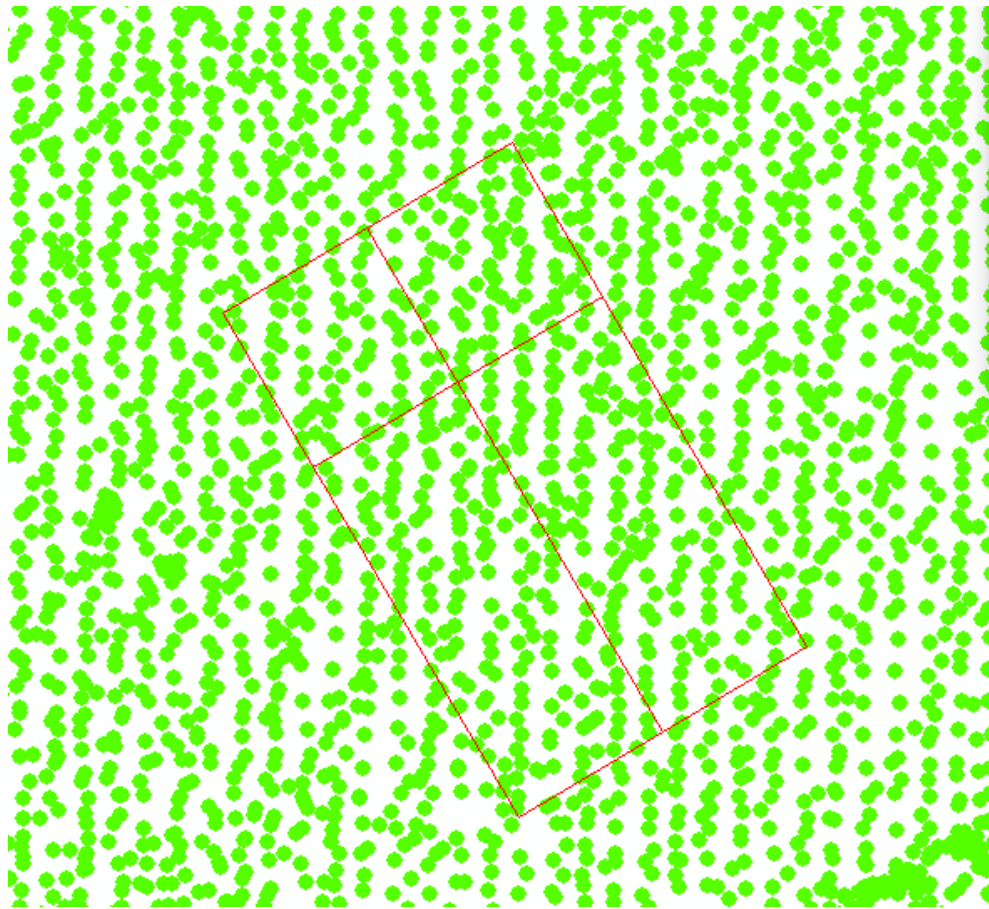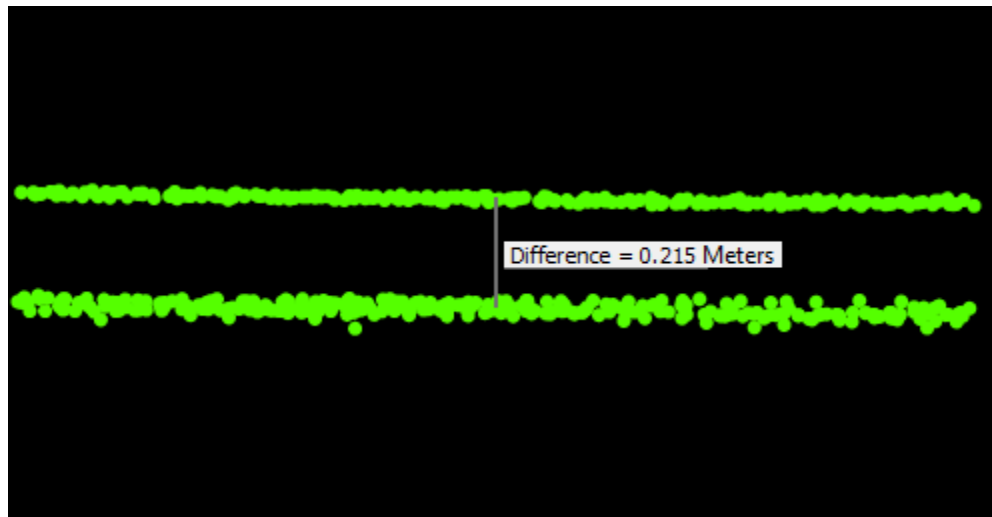
(b)

Figure 9. Comparison of point clouds from eastward and westward driving directions. Test area: 2 m x 1 m. (a) Top-down view, (b) vertical profile view.
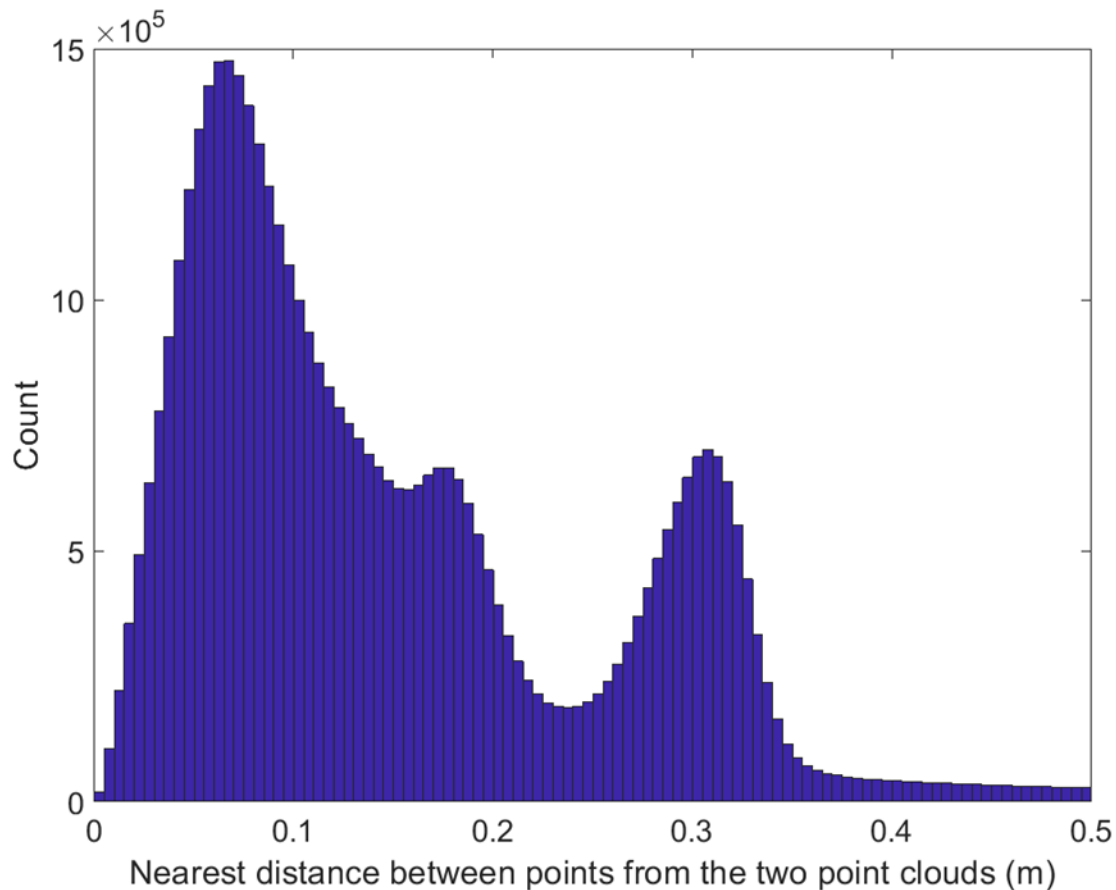
Figure 10. Histogram of the nearest distances between points from the east- and west-driving directions point clouds.

In total, three sources of geometric errors have been identified: 1) different channels or beams within a given sensor, 2) different sensors, and 3) different acquisition times (from eastward and westward driving directions). The first two sources of errors are related to the hardware and relatively constant over time. As a result, their errors can be reduced by simply averaging. The third source of errors are less predictable and need a data-dependent approach to reduce.

I used the Iterative Closest Point (ICP) algorithm to reduce the mismatch between the eastward and westward point clouds. This algorithm was first introduced by Chen and Medioni (1992) and Besl and McKay (1992). It fixes one point cloud as the reference (or target) and transforms the other (called source) point cloud to match the target point cloud. The algorithm iteratively performs the following:

1) Find the nearest point in the target point cloud for every point in the source point cloud;
2) Estimate the transformation matrix (including rotation and translation) based on the criteria of minimizing the average distance between the two point clouds,
3) Transform the source point cloud using the estimated transformation matrix.

The iterations will stop when either a maximum number of iterations have reached or the differences in the transformation (mainly translation distance and rotation angle) between two iterations are smaller than the predefined tolerance levels. In this study, I set the maximum number of iterations to 1000, translation distance tolerance to 0.001 m, rotation angle tolerance to 0.005 degrees.

4.2. Registration of mobile and airborne LiDAR data

The airborne and mobile LiDAR data were collected at different years and time, which can lead to different GNSS positioning solutions due to the differences in satellite configurations. Moreover, the quality of the hardware (inertial measurement units, GNSS receiver, laser range finder) differs. The integration and calibration of these hardware were conducted by different manufacturers and providers. The resulting point clouds could also be georeferenced to different vertical datums. Therefore, systematic differences could exist between mobile and airborne LiDAR data. Figure 11 shows an example area where the two point clouds have a horizontal shift of 2-3 m and a vertical shift of about 0.5 m.
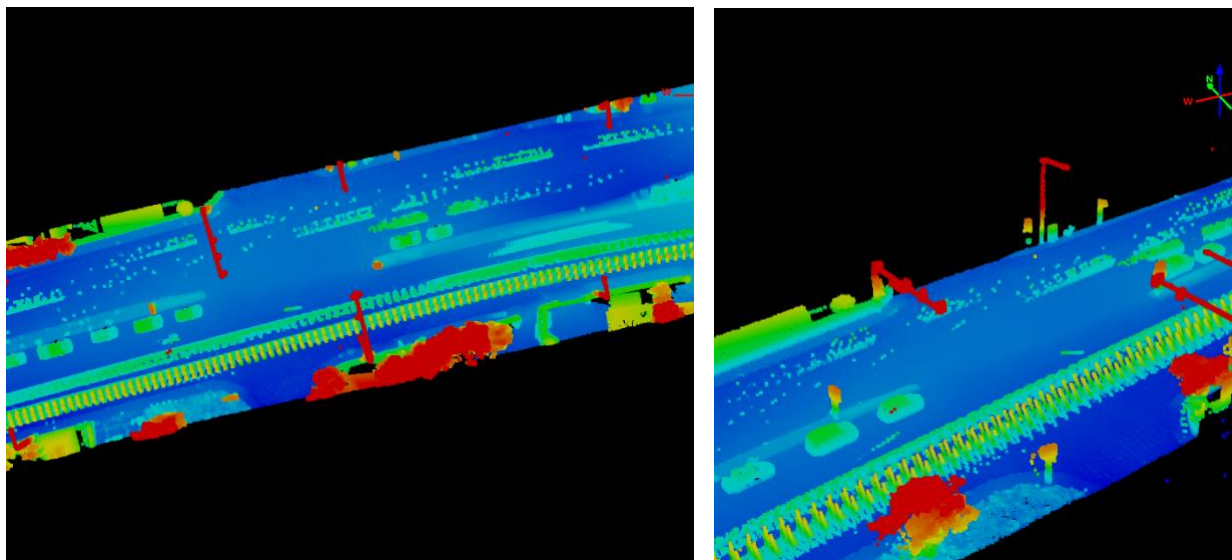
(a)
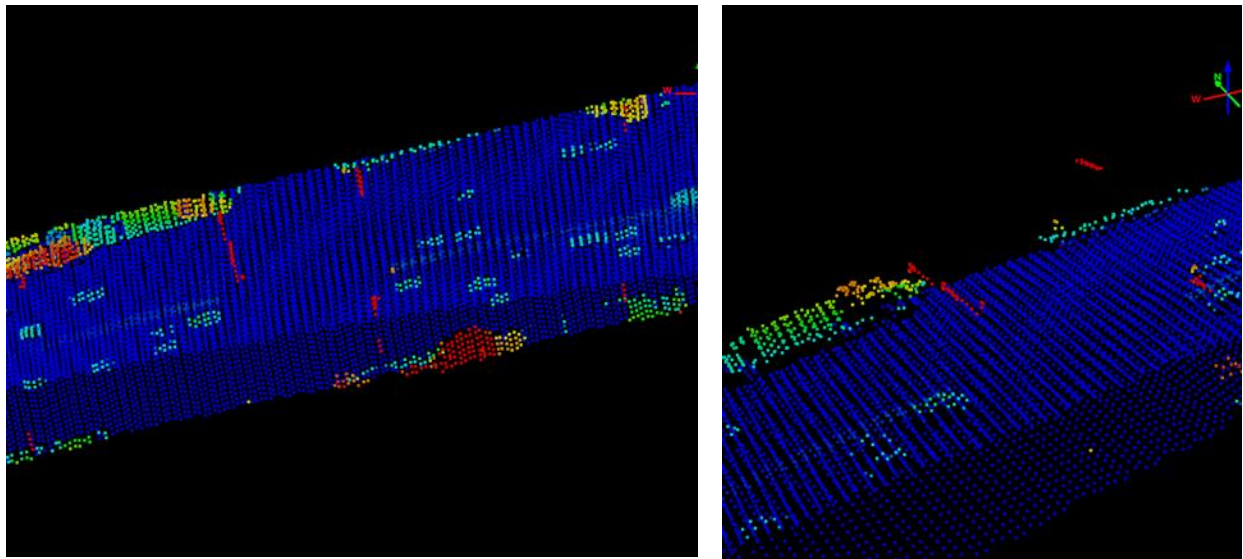
(b)
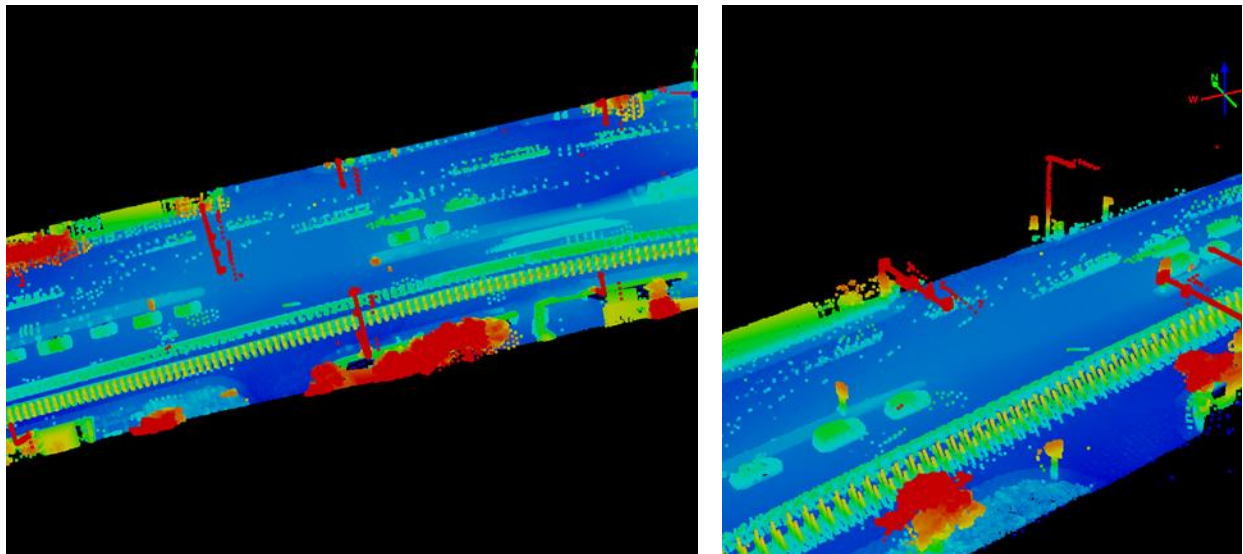
(c)

Figure 11. Comparison of mobile and airborne LiDAR data. (a) mobile LiDAR, (b) airborne LiDAR, and (c) both mobile and airborne LiDAR data.

I used the ICP algorithm to register the mobile and airborne LiDAR data. During this process, the airborne LiDAR data were used as the target or reference while the mobile LiDAR data was used as the source for transformation. Because airborne LiDAR systems use GNSS receivers mounted on the airplane instead of on the vehicle, the airborne GNSS signals are not subject to multipath or loss issues caused by building or tree obtrusions. Moreover, the airborne IMU and laser sensor is much more expensive and has better quality. The down side of airborne LiDAR data is that they are collected over a longer range, which can amplify errors in attitude, range, and

position. However, airborne LiDAR data are collected over a short period in general and the data are at least more consistent over large areas. Therefore, I used the airborne LiDAR data as the reference for registration and set the maximum number of iterations to 100, translation distance tolerance to 0.01 m, rotation angle tolerance to 0.05 degrees. Note that these parameters are smaller than the ones for registering different mobile LiDAR data. This is because the airborne LiDAR data have sparser point density and the registration is easier to converge. Figure 12 shows an example of registration between mobile and airborne LiDAR data.
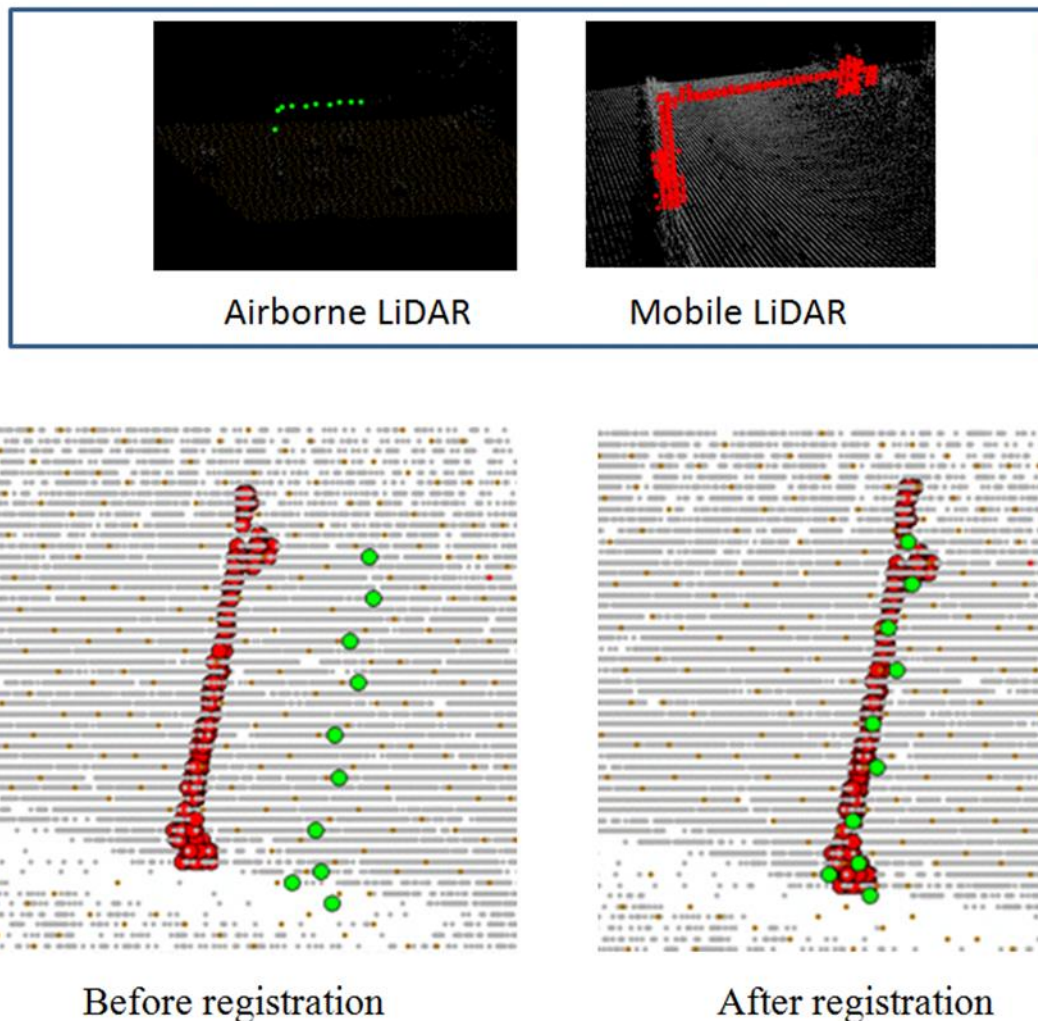
Figure 12. Co-registration of airborne and mobile LiDAR data. The top row shows the traffic light in airborne LiDAR (green) and mobile LiDAR (red) data in 3D. The bottom row shows the traffic light before and after registration in 2D.

4.3. Strategies for improving the speed and quality of registration

In the aforementioned procedure, one of the main challenges is the large data volume of mobile LiDAR data, which can lead to very long (days to weeks) processing time and poor results for registration. I used several strategies to address this issue. First, note that the further

away from the driving lane, the sparser the mobile LiDAR point cloud. This is more severe off the street due to the blockage of laser energy by objects, especially buildings. The points off the street are not useful in the registration process. Therefore, I manually digitized the center line of the road, created a 20-m buffer around the line, and selected only the mobile LIDAR data within the buffer for registration (Figure 13).

Second, I further reduced the mobile LiDAR data by creating 10 cm by 10 cm by 10 cm voxels and calculated the average coordinates of points within each voxel. The centroids (or the average coordinates) of voxels are saved as new point clouds for registration. This can not only substantially reduce the data volume and increase the speed for registration but also reduce the geometric errors associated with the use of different laser beams and different sensors, as discussed in section 4.1.

Figure 13. Subsetting the mobile LiDAR data near the street. (Top): the road center line and its 20-m buffer, (Bottom left) the original mobile LiDAR data, (Bottom right) the mobile LiDAR data within the buffer.

4.4. Filtering ground returns of point cloud and generating DTM

The raw LiDAR point cloud are just points with X, Y, Z coordinates and some ancillary information such as intensity and GPS time, without class information designating whether it is from a particular type of surface (for example, ground, building, or trees). As shown in Figure 11 (a) and (b), both mobile and airborne LiDAR data records objects on the earth surface such as building, trees, and cars. To generate DTM from LiDAR data, the points from the ground have to be classified or filtered. Although ground returns have been filtered for airborne LiDAR data by the data provider, the mobile LiDAR data have not been done so yet.

I used the ArcGIS (ESRI, Redlands, CA) 10.6 and its "Classify LAS Ground" tool of the 3D Analyst Extension to filter the ground returns. The tool provides three ground detection methods: standard, conservative, and aggressive. The conservative method removes the most points from surface objects such as building, trees, cars, but it has the risk of removing many ground points as well. The aggressive method keeps the most ground returns, but it has the tendency of including many points from aboveground objects (e.g., shrubs) as ground returns. The standard method is a method that balances both the omission and commission errors of ground returns. I first ran the standard method to derive an initial set of ground returns, and then executed the aggressive method to extract more ground returns from the initial ground returns. I found such a procedure can relatively well remove all aboveground object points and at the same time retaining ground returns from fine features such as road curbs captured in the mobile LiDAR data. The filtered ground returns were interpolated to a DTM raster using the "LAS Dataset to Raster" tool of ArcGIS. Because of the very dense point density of mobile LiDAR data, a simple binning algorithm was used to interpolate the point cloud to raster. Such an algorithm takes the average elevation of LiDAR ground points within each cell (which was set to 0.2 m by 0.2 m) as the output. When no ground returns fall in a cell, its elevation is linearly interpolated from the surrounding cells. Figure 14 shows the DTM generated from the fusion of mobile and airborne LiDAR data along the street and compares it with the one from airborne LIDAR data only. Figure 15 shows the DTM for the larger watershed.
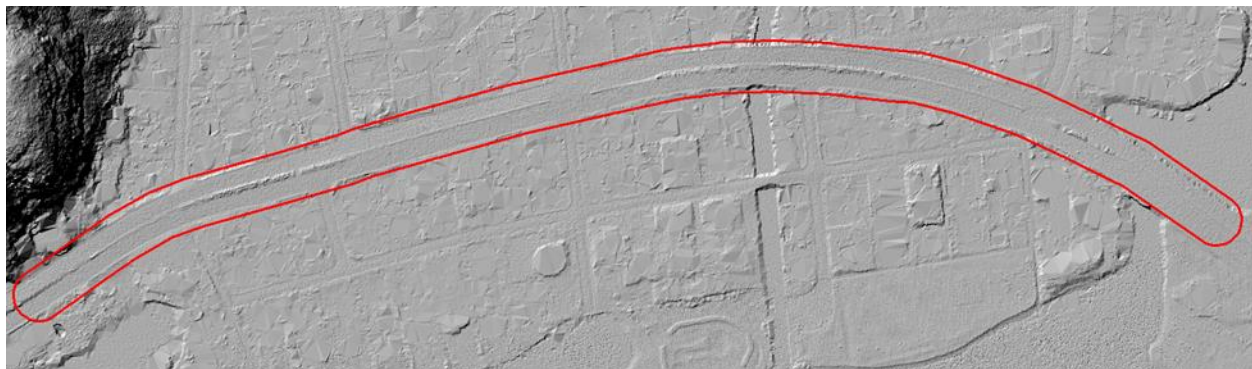
(a)

(b)
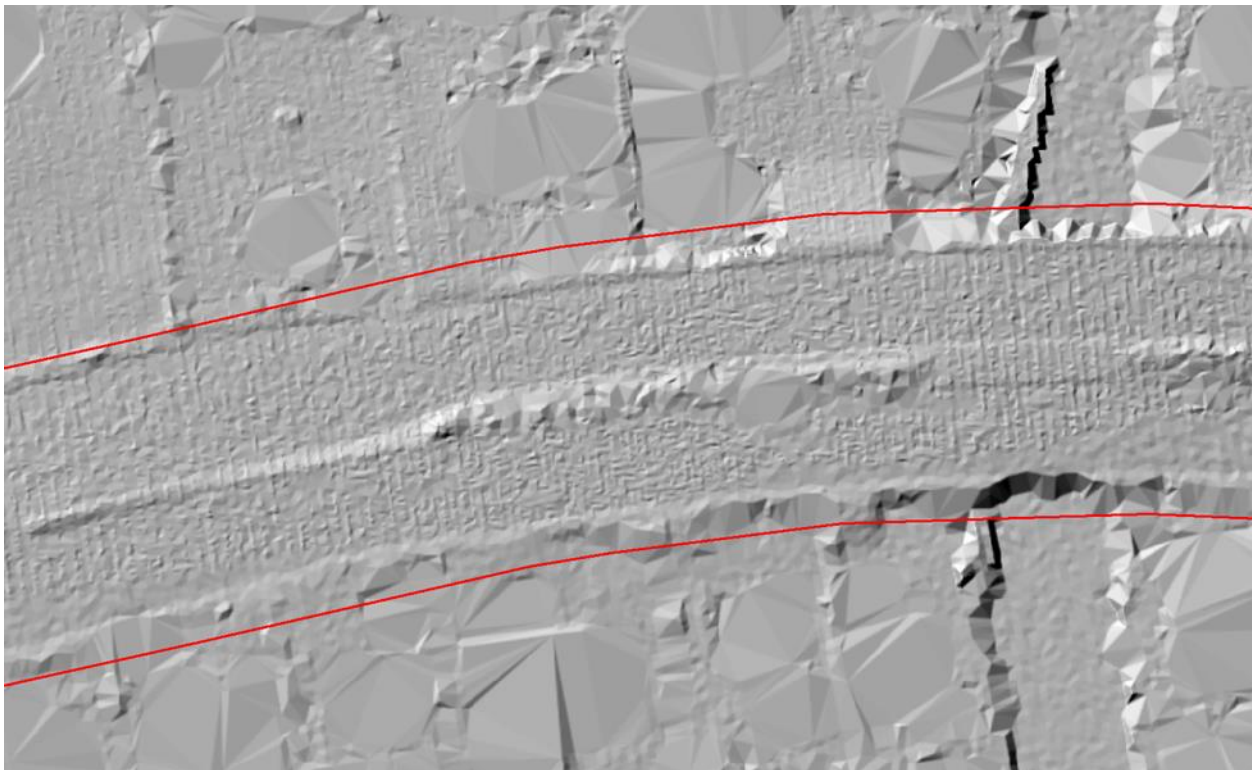
(c)
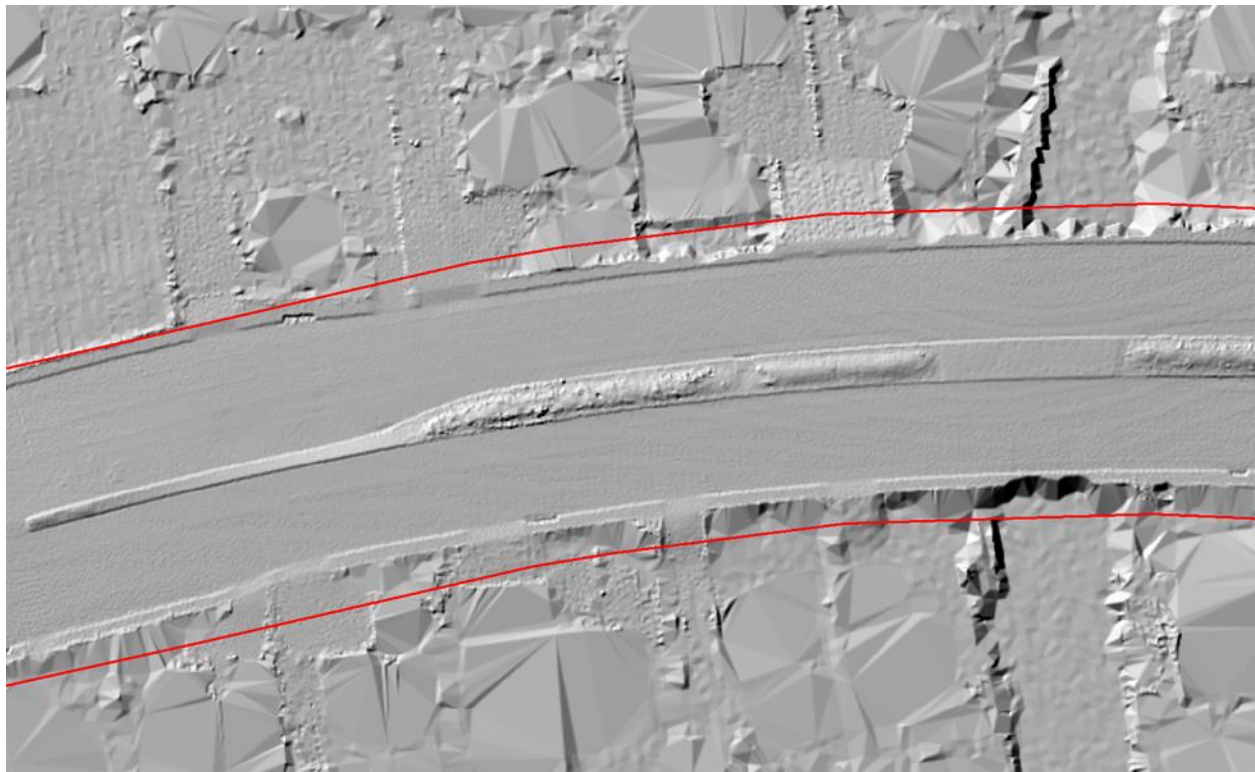
(d)

Figure 14. Comparison of DTMs generated from airborne LiDAR only ((a) and (c)) and from the fused airborne and mobile LiDAR data ((b) and (d)). The red polygon indicates the area for comparing DTMs from airborne and mobile LiDAR data. The black box indicates a sub area shown in (c) and (d).
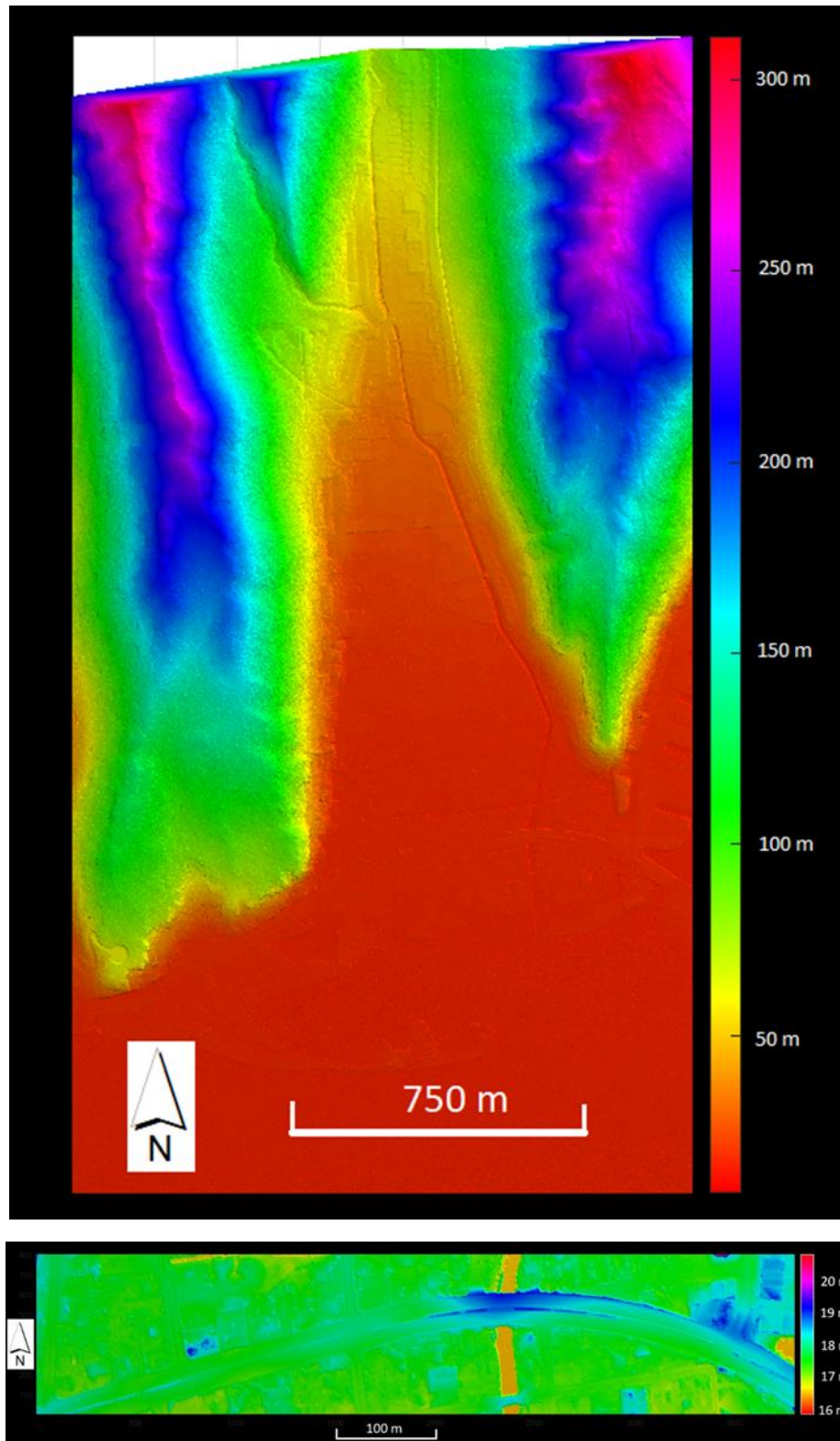
Figure 15. Watershed-level DTM by fusing airborne and mobile LiDAR data. (Top) the whole watershed, (Bottom) a sub-area (green box in the above picture) of the study area.

4.5 Inundation analysis

The airborne LiDAR data used in this study were not vertically georeferenced to a local tidal datum. The average elevation of the laser points from the water surface is around 16.5, instead of zero, meters. To conduct inundation analysis above sea-level as measured in the airborne LiDAR data, I chose the water surface in the airborne LiDAR data as the reference and then used the bathtub approach (Cooper and Chen, 2013; Cooper et al., 2013a, 2013b) to map the inundated areas.

Figure 16 shows a comparison of the inundated areas over a road segment when water arises by 1 m, 1.1 m, 1.3 m, 1.5 m, 1.7 m, and 2 m above the reference level. It is shown that the inundate maps from the airborne LiDAR data only and from the fused mobile and airborne LiDAR data are not drastically different. This is expected because the mobile LiDAR data were registered to the airborne LiDAR data.

1 m above sea-level (using DTM from airborne lidar)
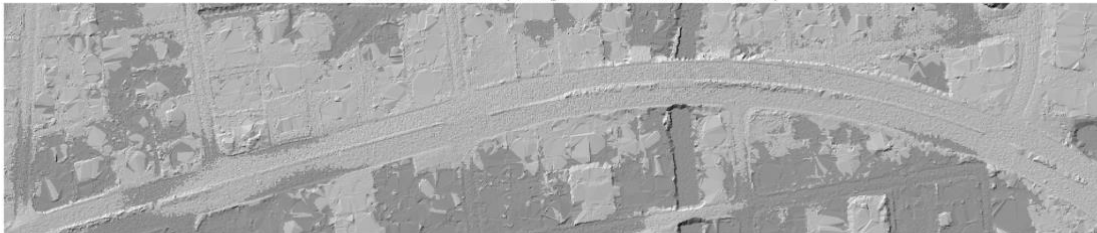
1 m above sea-level (using DTM from mobile+airborne lidar)
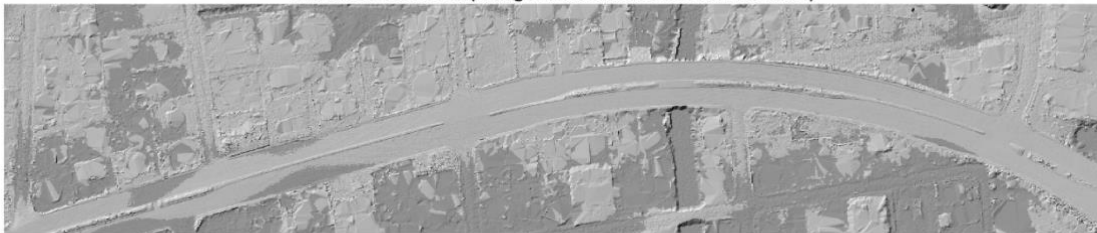
1.1 m above sea-level (using DTM from airborne lidar)
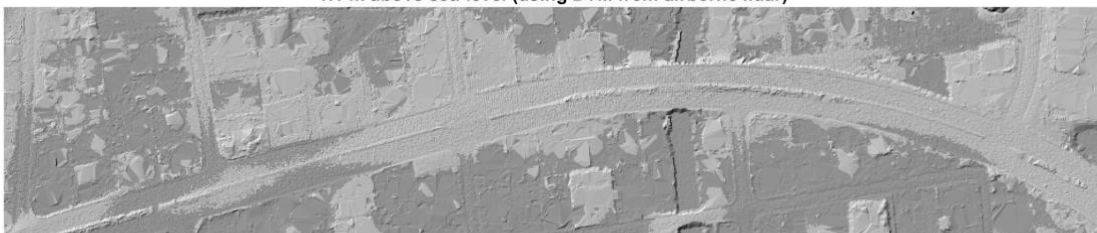
1.1 m above sea-level (using DTM from mobile+airborne lidar)
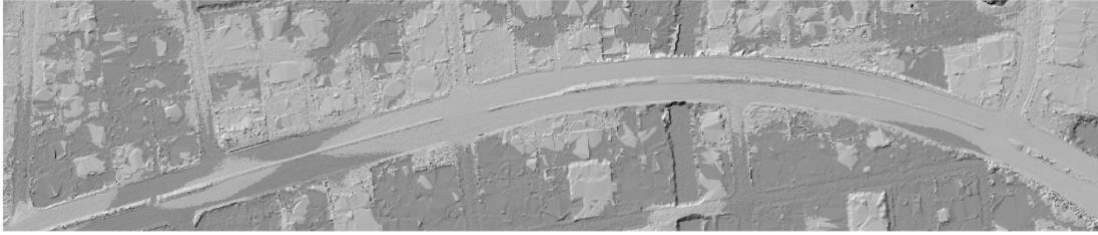
1.3 m above sea-level (using DTM from mobile+airborne lidar)
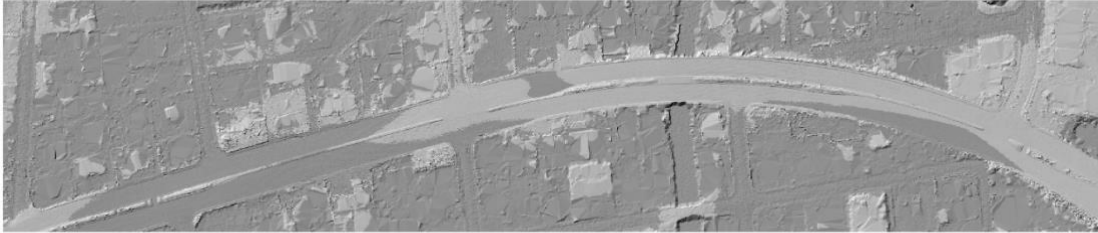
1.3 m above sea-level (using DTM from airborne lidar)

1.5 m above sea-level (using DTM from airborne lidar)

1.5 m above sea-level (using DTM from mobile+airborne lidar)
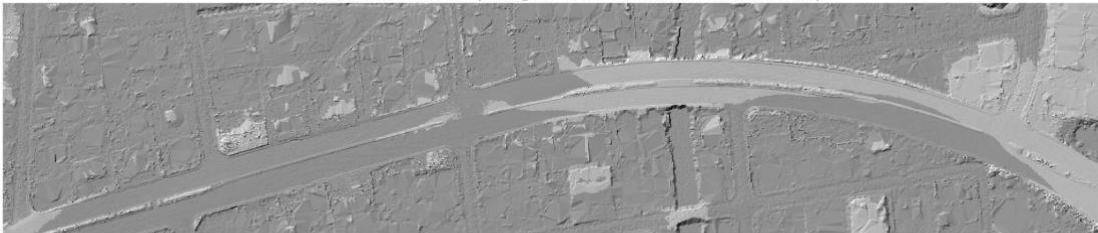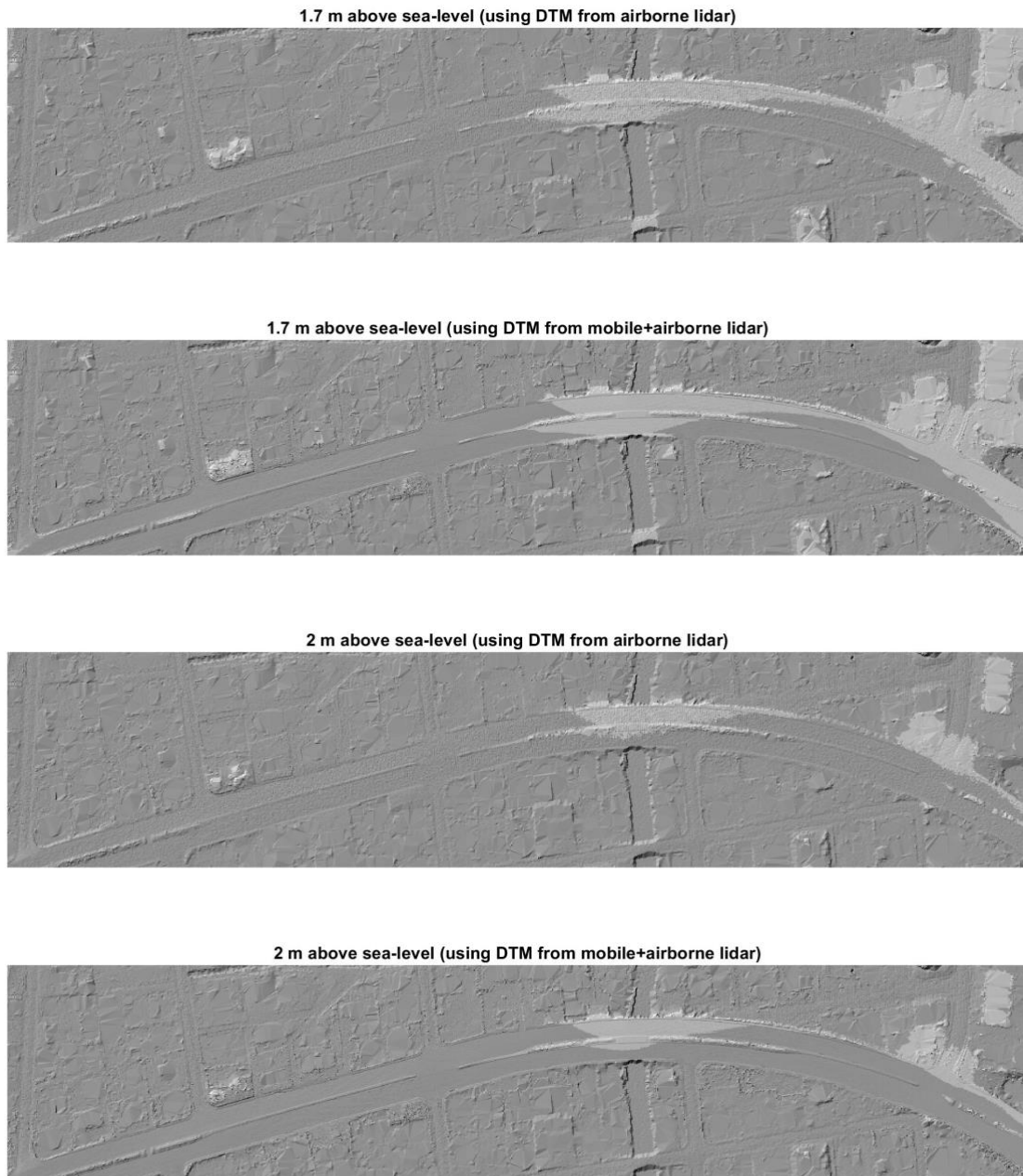
Figure 16. Comparison of inundation maps from airborne LiDAR only and from the fused mobile and airborne LiDAR data.

As shown in the details of the maps (Figure 17), the inundation maps from the fused LiDAR data are more continuous and smooth than the airborne LiDAR data.
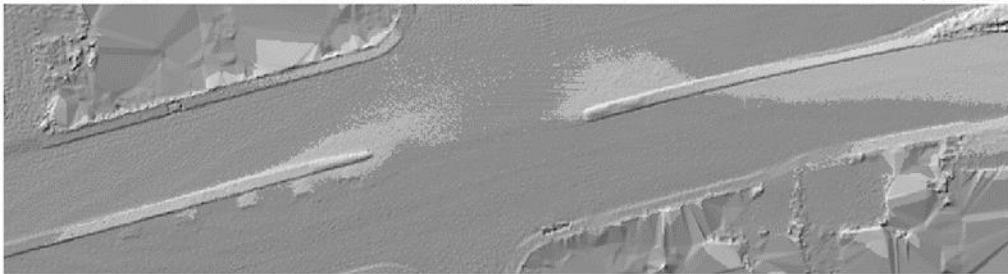
Figure 17. Comparison of inundation maps' details. (Top) from airborne LiDAR data only, (Bottom) from fused mobile and airborne LiDAR data.

5. Summary

Mobile LiDAR has emerged as a state-of-the-art technology for mapping urban infrastructure and environment (Wang et al., 2019). However, the use of mobile LiDAR for analyzing the roadway vulnerability to inundation is still in its infancy. This project is one of the first studies to investigate the use of airborne and mobile LiDAR data for road inundation analysis. Several significant findings can be derived from this study:

1) although mobile LiDAR data have a point density of several magnitudes higher than the airborne LiDAR, its geometric errors are relatively large and in the order of tens of centimeters,

2) the geometric errors of mobile LiDAR data can be attributed to the use of different laser beams (or channels) in a given laser sensor, the use of different laser sensors in a single vehicle, and the use of data collected from different times. In particular, mobile LiDAR data collected from different times have relatively large geometric discrepancy due to the GNSS signal variability and obtrusion over urban areas,

3) large geometric mismatch (in the order of several meters) exists between mobile LiDAR and airborne LiDAR data,

4) an efficient and accurate algorithm to register different LiDAR data and reduce their geometric errors is the key to use them for precise environmental mapping. The Iterative Closest Point (ICP) algorithm is a relatively effective approach for LiDAR data registration. However, methods are needed to preprocess the data to increase its speed and accuracy.

5) the combination of airborne and mobile LiDAR data is a promising and effective strategy for mapping detailed road infrastructure and conducting inundation analysis. The fused DTM derived from the combined LiDAR data carries the geometric consistency associated with airborne LiDAR data and the spatial details of mobile LiDAR data, which can help more informed decision in transportation infrastructure planning and management.

In the future, more research is needed to test and improve the methods developed in this study over lager study areas with varying roads conditions.

References

Besl, P.J., & N.D. McKay (1992). A Method for Registration of 3-D Shapes. IEEE Transactions on Pattern Analysis and Machine Intelligence. 14 (2): 239–256

Chen, Y., & G. Medioni (1992). Object modelling by registration of multiple range images. Image Vision Comput. 10 (3): 145–155

Cooper, H. M., & Chen, Q. (2013). Incorporating uncertainty of future sea-level rise estimates into vulnerability assessment: A case study in Kahului, Maui. Climatic change, 121(4), 635-647.

Cooper, H. M., Chen, Q., Fletcher, C. H., & Barbee, M. M. (2013a). Assessing vulnerability due to sea-level rise in Maui, Hawai ʻi using LiDAR remote sensing and GIS. Climatic Change, 116(3-4), 547-563.

Cooper, H. M., Fletcher, C. H., Chen, Q., & Barbee, M. M. (2013b). Sea-level rise vulnerability mapping for adaptation decisions using LiDAR DEMs. Progress in Physical Geography, 37(6), 745-766.

Fletcher, C., Boyd, R., Neal, W. J., & Tice, V. (2010). Living on the shores of Hawaii: Natural hazards, the environment, and our communities. University of Hawai'i Press.

Gesch, D. B. (2009). Analysis of lidar elevation data for improved identification and delineation of lands vulnerable to sea-level rise. Journal of Coastal Research, 49-58.

Hawaiʻi Climate Change Mitigation and Adaptation Commission (HCCMAC). (2017). Hawaiʻi Sea Level Rise Vulnerability and Adaptation Report. Prepared by Tetra Tech, Inc. and the State of Hawaiʻi Department of Land and Natural Resources, Office of Conservation and Coastal Lands, under the State of Hawaiʻi Department of Land and Natural Resources Contract No: 64064.

Onat, Y., Francis, O. P., & Kim, K. (2018). Vulnerability assessment and adaptation to sea level rise in high-wave environments: A case study on O'ahu, Hawai'i. Ocean & Coastal Management, 157, 147-159.

Wang, Y., Chen, Q., Zhu, Q., Liu, L., Li, C., & Zheng, D. (2019). A Survey of Mobile Laser Scanning Applications and Key Techniques over Urban Areas. Remote Sensing, 11(13), 1540.

Yin, J., Yu, D., Lin, N., & Wilby, R. L. (2017). Evaluating the cascading impacts of sea level rise and coastal flooding on emergency response spatial accessibility in Lower Manhattan, New York City. Journal of Hydrology, 555, 648-658.

PSR Pacific Southwest Region UTC
University Transportation Center

Data Management Plan

Products of Research

The product includes: 1) a Digital Terrain Model (DTM; 0.2 m resolution) that integrates airborne and mobile lidar (Light Detection and Ranging) data, and 2) a shapefile that shows the road segment of the Kamehameha Highway where mobile lidar data were available and used for generating the DTM. The airborne lidar were collected by NOAA in 2013 and the point density is 2.5 points/m^2. The mobile lidar data were collected by Hawaii DOT (Department of Transportation) with the Mandli DVX system. The system includes Velodyne HDL-32 LiDAR sensors (each with a pulse rate of 700,000 points per second, range of 100 m, relative positive accuracy of < 2 cm for 1 sigma at 25 m, vertical angular resolution of 1.33°, wavelength of 905 nm), which are mounted at the two rear corners of the vehicle. The point density is 3334.4 points/m^2.

Data Format and Content

The DTM is in geotiff (.tif) format while the shapefile is in ArcGIS shapefile (.shp) format. DTM is a raster model that represent the elevation of bare earth, excluding aboveground objects such as trees, building, electric poles, traffic signs, etc. The shapefile is the centerline of the road segment corresponding to the mobile lidar data used in the study.

Both data are in the projection of UTM (Universal Transverse Mercato) Zone 4N with the datum of NAD (North America Datum) 1983 (2011). The vertical elevation is in ellipsoid instead of orthometric heights.

Data Access and Sharing

The data can be accessed at the following DOI link: https://doi.org/10.7910/DVN/1VT6FZ

Reuse and Redistribution

The data can be reused and redistributed by the general public.

Pacific Southwest Region UTC
University Transportation Center